Electronic Supplementary Material (ESI) for Nanoscale Advances.

Interfacial complexation driven three-dimensional assembly of cationic phosphorus dendrimers and graphene oxide sheets

Nadia Katir, Anass Benayad, Denis Rouchon, Nathalie Marcotte, Nabil Brahmi, Jean Pierre Majoral, Mosto Bousmina and Abdelkrim El Kadib.

S1: Experimental section

S1a: Characterization of materials.

General The manipulations were carried out with standard high-vacuum and dry-argon techniques. Solvents were dried and distilled according to standard procedures. All reagents were purchased from Sigma-Aldrich or Strem and were used without further purification. $\mathbf{DG_n}$ were synthesized using published procedures.[ref] NMR spectra were recorded with Bruker AV 400 and HD 400 spectrometers. All spectra were measured at 25°C in the indicated deuterated solvents. References for NMR chemical shifts are H_3PO_4 (85%) for ^{31}P NMR, and $SiMe_4$ for ^{1}H and ^{13}C NMR spectroscopy.^{1}H, ^{13}C and ^{31}P chemical shifts (δ) are reported in ppm and coupling constants (*J*) are reported in Hertz (Hz). ^{13}C and ^{31}P CP MAS NMR spectra were acquired on a Bruker Avance 400 WB spectrometer operating at 100 MHz and 162 MHz respectively under cross-polarization conditions. Fourier transformed infrared (FTIR) spectra were obtained with a Perkin-Elmer Spectrum 100FT-IR spectrometer on neat samples (ATR FT-IR). X-ray powder diffraction (XRD) patterns were recorded on a D8 Advance Bruker AXS system using CuKα radiation with a step size of 0.02° in the 2θ range from 0.45 to 87° for WAXS (geometry : Bragg- Brentano, θ/2θ mode). DRUV spectra were measured in the 200–800 nm range using spectralon as the reference on a Perkin-Elmer Lambda 1050 spectrometer equipped with an integrating sphere (Lapshere, North Sutton, USA). The XPS measurements were performed on a VersaProbe-II tool from ULVAC-Phi using a focused monochromated Al Ka radiation (1486.6 eV). The spectrometer was calibrated using the photoemission lines of gold (Au 4f7/2 emission at 83.9 eV, with reference to the Fermi level). The core level peaks and the survey spectra were recorded with a constant pass energy of 23.3 eV and 117.9 eV, respectively. All spectra were recorded using electron and argon charge neutralizer guns to minimize the surface charging effect that may occur at the insulating powder surface during the photoemission process. All spectra were calibrated using the contamination carbon C 1s emission at 284.8 eV. The XPS spectra were fitted using Multipak V9.1 software in which a Shirley background was assumed, and the peak fittings of the experimental spectra were defined by a combination of Gaussian (80%) and Lorentzian (20%) distributions. Raman spectra were recorded in the backscattering geometry using a In-Via Renishaw Raman spectrometer. The light was focused onto the sample surface thanks to a 100 x (0.85 NA) short working objective lens, resulting in a spot diameters around 0.8 μm. Our measurements were carried out using excitation wavelength l at 532 nm with a typical laser power of ~0.5 mW. Raman spectroscopy was used to observe the structural modifications for each sample.

S1b: Synthesis and characterization of the poly(phosphorhydrazone) dendrimers ending with ammonium groups DG_n: [1]

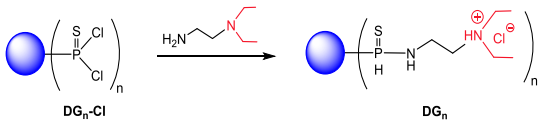

DG_n-Cl DG_n

N,N-Diethylethylenediamine (n = 1, 93 mL, 0.66 mmol; n = 2, 71 mL, 0.5 mmol; n = 3, 68 mL, 0.48 mmol; n = 4, 61 mL, 0.43 mmol) was added dropwise by syringe with strong stirring to a solution of dendrimer (**DG_n-Cl**] (100 mg; n = 1, 55 mmol; n = 2, 21 mmol; n = 3, 10 mmol; n = 4, 4.5 mmol) in distilled THF (15 mL). After stirring overnight at room temperature, the solvent was removed by filtration. The white powder was washed with distilled THF (2 X 20 mL) and evaporated to dryness. The protons produced during the coupling reaction were trapped by the terminal tertiary amine residues; consequently **DG_n** dendrimers were obtained as chlorohydrate derivatives.

Dendrimer DG_1:

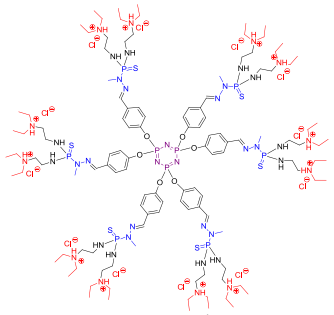

Yield 80%; $^{31}P\{^1H\}$ NMR (CD_3OD): δ.7.9 (P_0), 69.6 (P_1); ^1H NMR ([D_6]DMSO): δ.1.3 (t, $^3J_{HH}$.= 6.3 Hz, 72H; CH_2CH_3), 3.0 ± 3.5 (m, 114H; CH_3-N-P_1, CH_2), 5.7 (br m, 12H; $^+$N-H), 7.1 (d, $^3J_{HH}$.= 8.4 Hz, 12H; C_0^2-H), 7.9 (s, 6H; CH-N), 7.9 (d, $^3J_{HH}$.= 8.4 Hz, 12H; C_0^3-H), 10.8 (br s, 12H; $^+$N-H); $^{13}C\{^1H\}$ NMR (CD_3OD): δ.9.7 (s, CH_2CH_3), 33.3 (d, $^2J_{CP1}$.= 10.3 Hz, CH_3-N-P_1), 37.9 (s, CH_2-N-P_1), 49.5 (s, CH_2CH_3), 53.9 (d, $^3J_{CP1}$.= 6.2 Hz, CH_2-CH_2-N-P_1), 122.6 (s, C_0^2), 129.8 (s, C_0^3), 135.0 (s, C_0^4), 139.3 (d, $^3J_{CP1}$ = 11.6 Hz, CH-N), 152.4 (d, $^2J_{CP0}$ = 7.3 Hz, C_0^1);

Dendrimer DG_2:

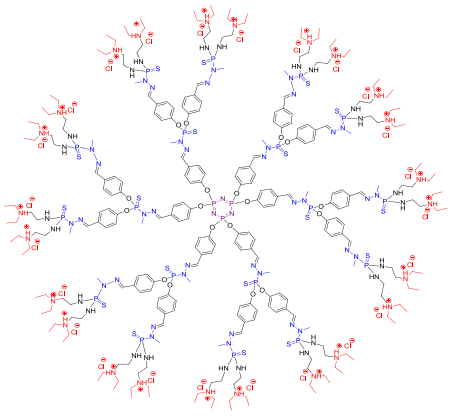

Yield 95%; $^{31}P\{^{1}H\}$ NMR (CD_3OD): δ 8.5 (P_0), 62.0 (P_1), 69.6 (P_2); ^{1}H NMR ([D_6]DMSO): δ 1.3 (brs, 144H; CH_2CH_3), 3.0-3.6 (m, 246H; CH_3-N , CH_2), 5.6 (br m, 24H; N-H), 7.0-7.4 (m, 36H; C_0^2-H, C_1^2-H), 7.7 - 8.2 (m, 54H; CH=N, C_0^3H, C_1^3H), 10.7 (brs, 24H; $^{+}$N-H); $^{13}C\{^{1}H\}$ NMR (CD_3OD): δ 9.6 (s, CH_2CH_3), 33.0 (d, $^{2}J_{CP2}$ = 10.6 Hz, CH_3-N-P_2), 34.2 (d, $^{2}J_{CP1}$ = 11.8 Hz, CH_3-N-P_1), 37.8 (s, CH_2-N-P_2), 49.2 (s, CH_2CH_3), 53.9 (d, $^{3}J_{CP2}$ = 6.3 Hz, CH_2-CH_2-N-P_2), 122.8 (s, C_0^2), 123.0 (d, $^{3}J_{CP1}$ = 3.0 Hz, C_1^2), 129.7 (s, C_1^3), 130.0 (s, C_0^3), 134.3 (s, C_0^4), 135.0(s, C_1^4), 139.1 (d, $^{3}J_{CP2}$ = 12.5 Hz, CH=N), 141.3 (d, $^{3}J_{CP1}$ = 15.4 Hz, CH=N),152.6 (d, $^{2}J_{CP1}$ = 7.3 Hz, C_1^1), 152.6 (s, C_0^1).

Dendrimer DG_3:

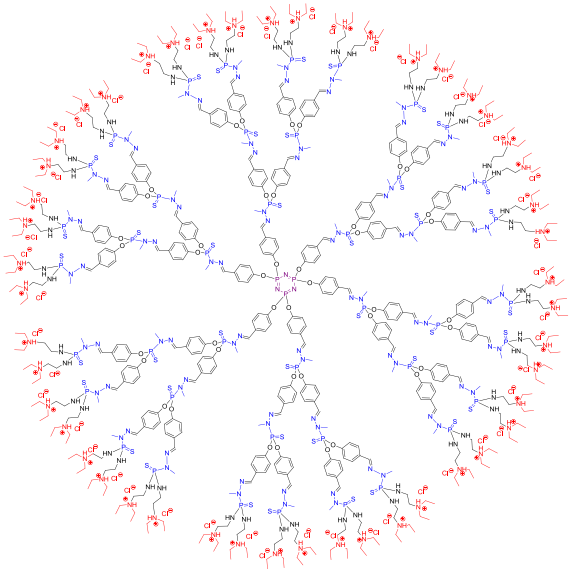

Yield 95%; $^{31}P\{^{1}H\}$ NMR (CD_3OD): δ 8.6 (P_0), 61.5 (P_1), 62.3 (P_2), 69.5 (P_3); ^{1}H NMR ([D_6]DMSO): δ 1.3 (br s, 288H; CH_2CH_3), 3.0 - 3.5 (br m, 510H; CH_3-N , CH_2), 5.7 (br s, 48H; N-H), 7.0 - 7.5 (br m, 84H; C_0^2-H, C_1^2-H, C_2^2-H), 7.7 - 8.2 (br m, 126H; CH=N, C_0^3-H, C_1^3-H, C_2^3-H), 10.8 (br s, 48H; $^{+}$N-H); $^{13}C\{^{1}H\}$ NMR (CD_3OD): δ 9.6 (s, CH_2CH_3), 33.1 (d, $^{2}J_{CP3}$ = 9.4 Hz, CH_3-N-P_3), 34.2 (m, CH_3-N-$P_{1,2}$), 37.6 (s, CH_2-N-P_3), 49.2 (s, CH_2CH_3), 53.7 (d, $^{3}J_{CP3}$ = 6.3 Hz, CH_2-CH_2-N-P_3), 123.2 (br s, C_0^2, C_1^2, C_2^2), 129.6 (br s, C_0^3, C_1^3, C_2^3), 134.0 (s, C_0^4, C_1^4), 134.8 (s,C_2^4), 139.0 (br s, C_2^4-CH=N), 141.4 (br s, CH=N), 152.4 (d, $^{2}J_{CP2}$ = 7.3 Hz, C_2^1), 152.8 (br s, C_0^1, C_1^1).

Dendrimer **DG$_4$**:

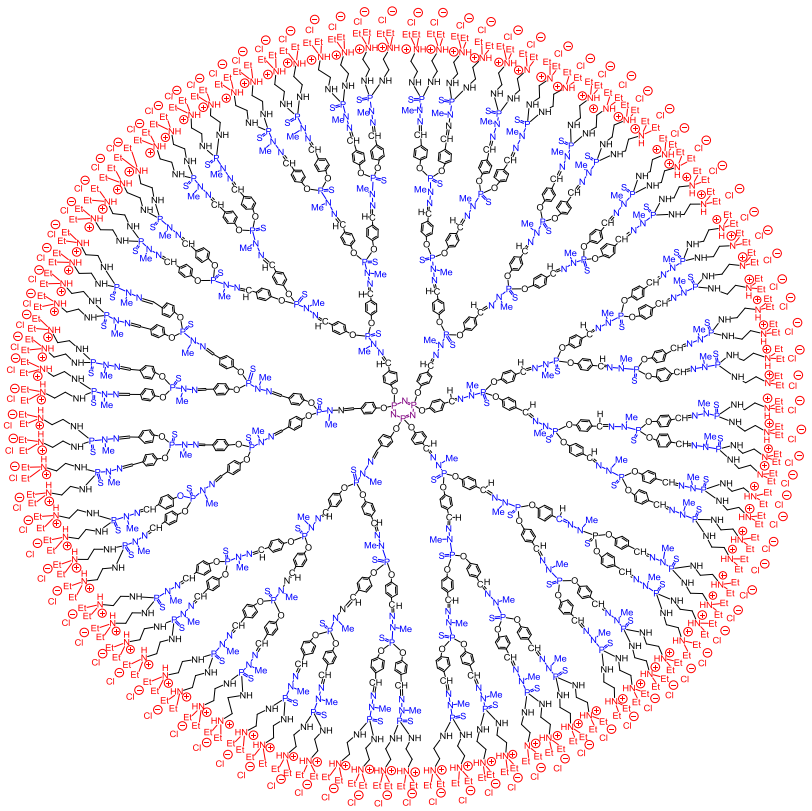

Yield 95%; $^{31}P\{^1H\}$ NMR (CD_3OD): δ 8.4 (P_0), 62.0 ($P_{1,2,3}$), 69.4 (P_4); ^1H NMR ([D_6]DMSO): δ 1.3 (brs, 576H; CH_2CH_3), 3.0 - 3.5 (m, 1038H; CH_3-N-$P_{1,2,3,4}$, CH_2), 5.6 (brs, 96H; N-H), 7.0 - 7.5 (brm, 180H; C_0^2-H, C_1^2-H, C_2^2-H, C_3^2-H), 7.7 - 8.2 (m, 270H; CH.N, C_0^3-H,C_1^3-H, C_2^3-H, C_3^3-H), 10.8 (brs, 96H; .N-H); $^{13}C\{^1H\}$ NMR (CD_3OD): δ 9.7 (s, CH_2CH_3), 33.2 (d, $^2J_{CP4}$ = 9.2 Hz, CH_3-N-P_4), 34.3 (d, $^2J_{CP}$ = 10.1 Hz, CH_3-N-$P_{1,2,3}$), 37.7 (s, CH_2-N-P_4), 49.2 (s, CH_2CH_3), 53.8 (d, $^3J_{CP4}$ = 5.5 Hz, CH_2-CH_2-N-P_4), 123.1 (brs, C_0^2, C_1^2, C_2^2, C_3^2), 129.7 (brs, C_0^3, C_1^3, C_2^3, C_3^3),134.2 (s, C_0^4, C_1^4, C_2^4), 134.9 (s, C_3^4), 139.2 (brs, C_3^4-CH=N), 141.5 (brs, CH=N), 152.5 (d, $^3J_{CP3}$ = 7.4 Hz, C_3^1), 153.0 (brs, C_0^1, C_1^1, C_2^1).

1. C. Loup, M. A. Zanta, A. M. Caminade, J. P. Majoral and B. Meunier, *Chem. Eur. J.*, 1999, 5, 3644-3650.

S2: DRIFT spectra

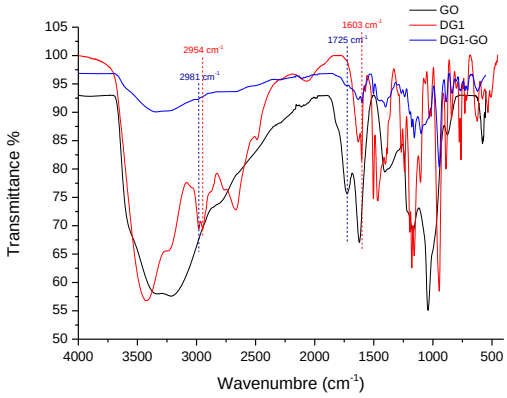

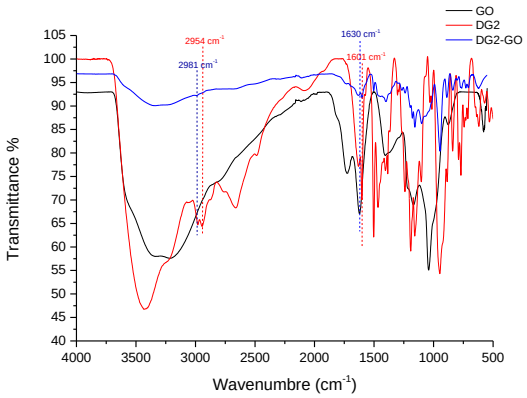

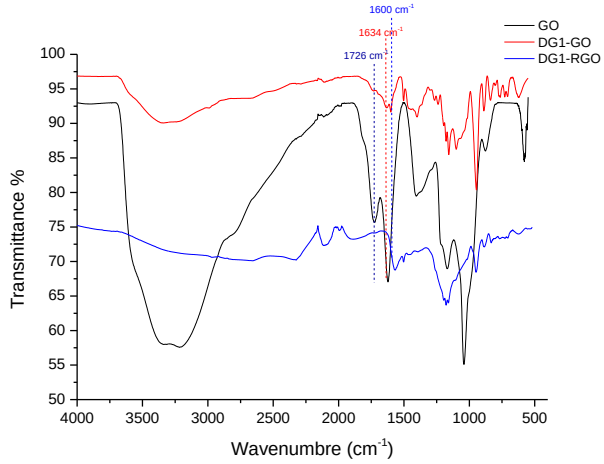

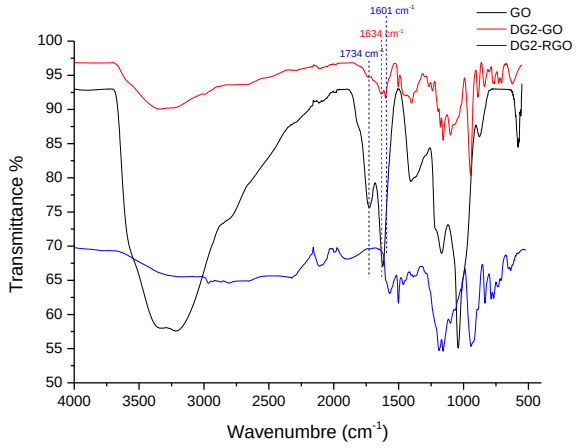

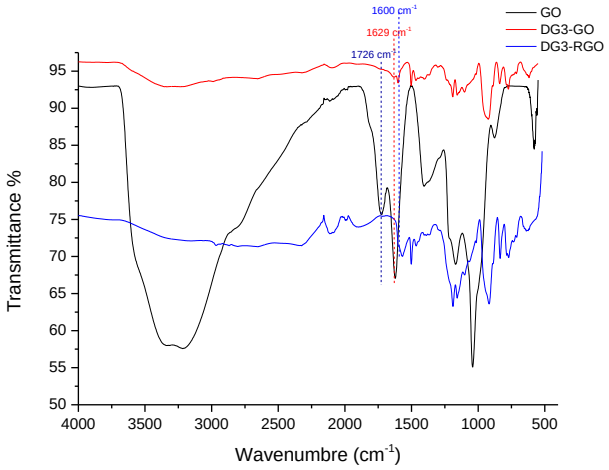

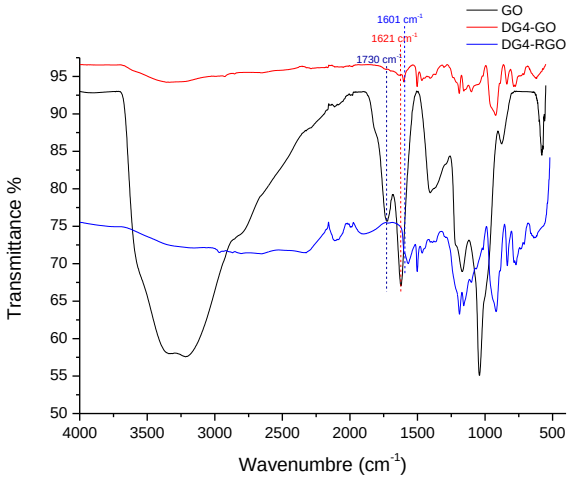

S3: CP ^{13}C and CP ^{31}P MAS NMR spectra

S3a: CP ^{13}C NMR spectra

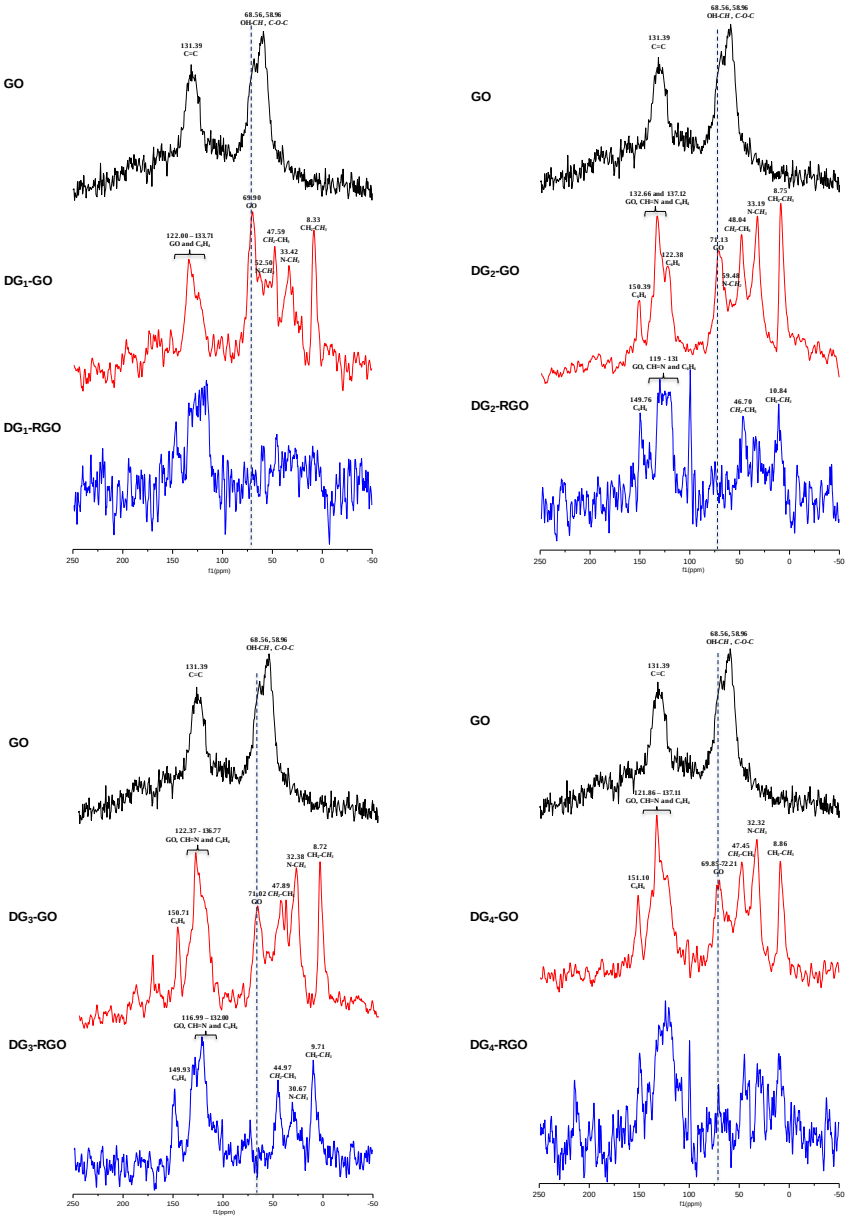

S3b: CP ^{31}P MAS NMR spectra

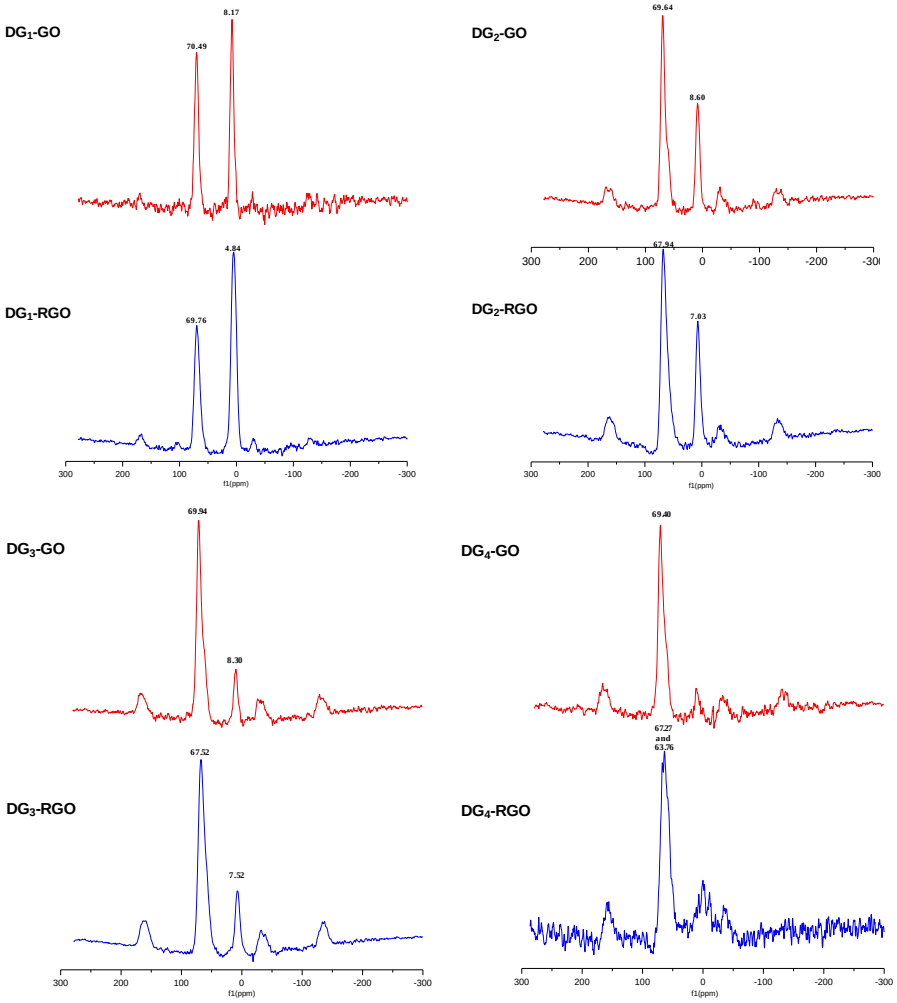

S4: XRD analysis

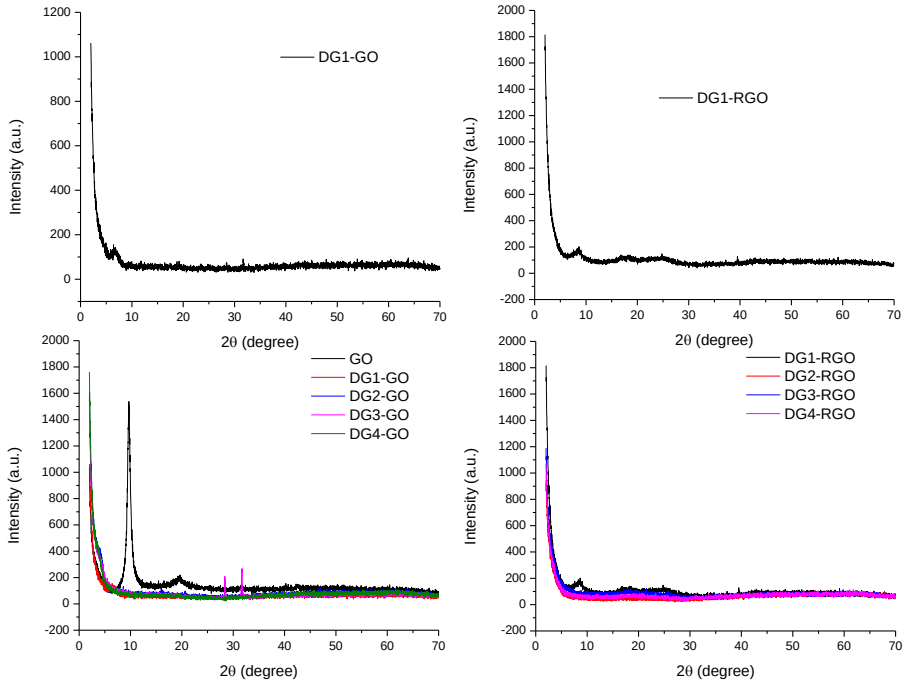

S5: SEM, TEM and EDX analysis of DG_4-GO

S5a: SEM analysis of DG_4-GO

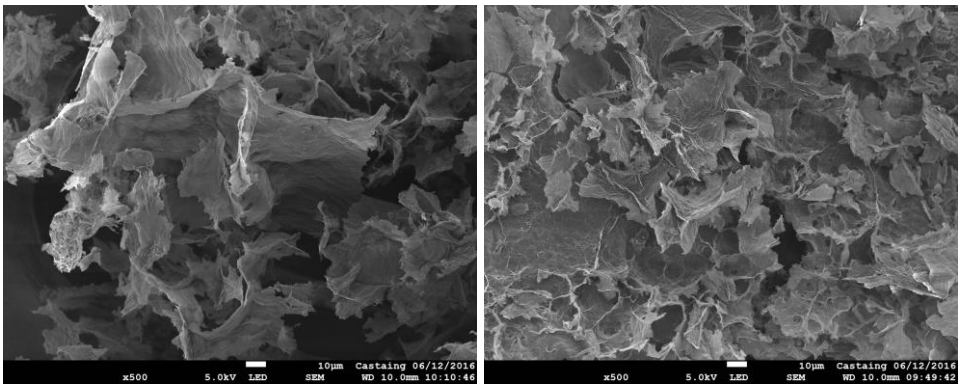

S5b: TEM analysis of DG_4-GO

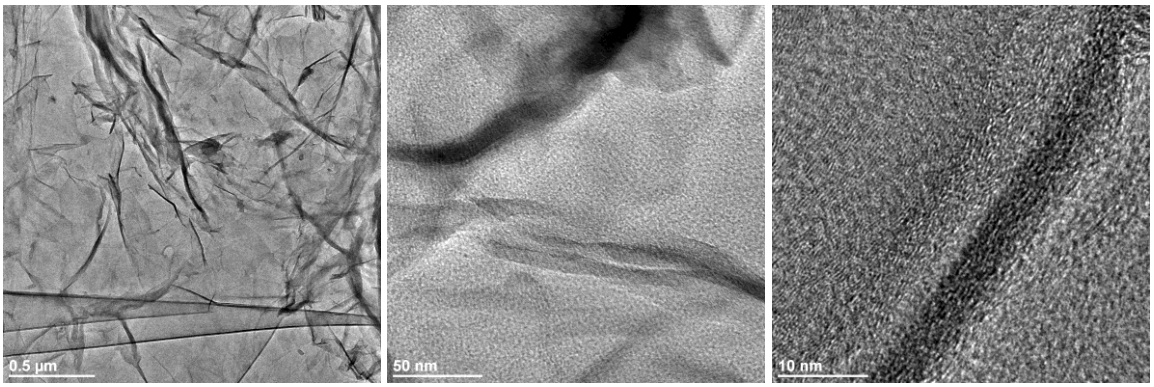

S5c: EDX analysis of DG_4-GO

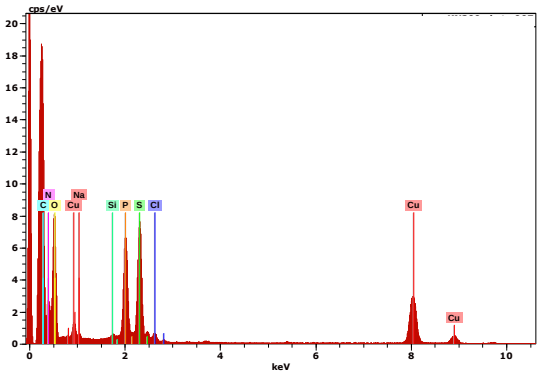

S6: UV spectra

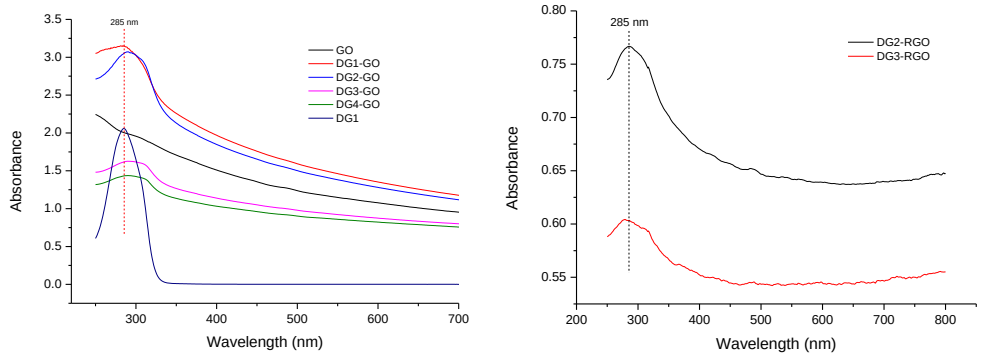

S7: SEM, TEM and EDX analysis of DG_4-RGO

S7a: SEM analysis of DG_4-RGO

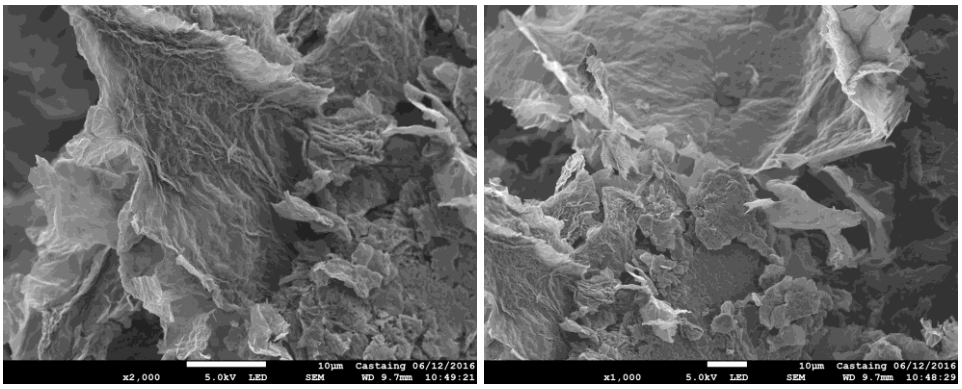

S7b: TEM analysis of DG_4-RGO

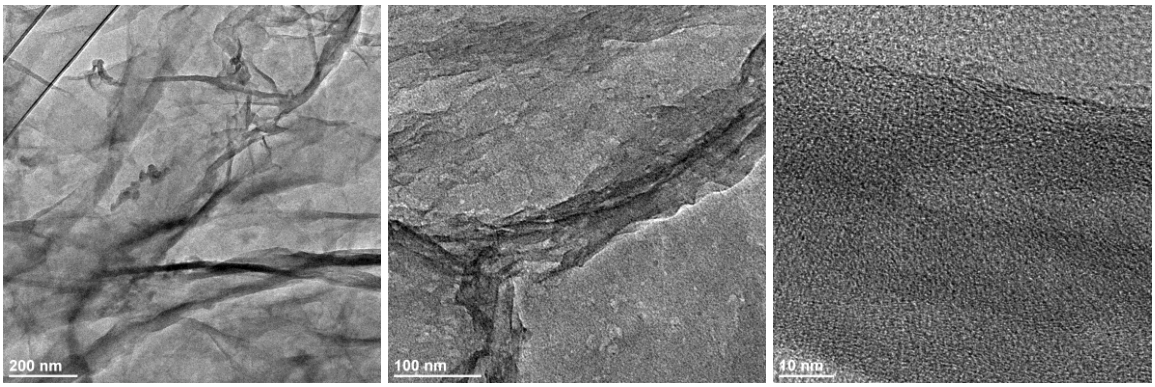

S7: EDX analysis of DG_4-RGO

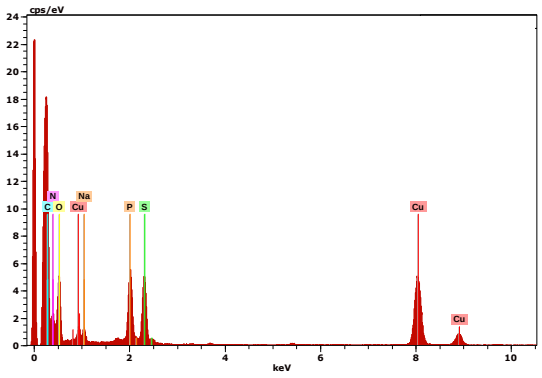

S8: RAMAN analysis:

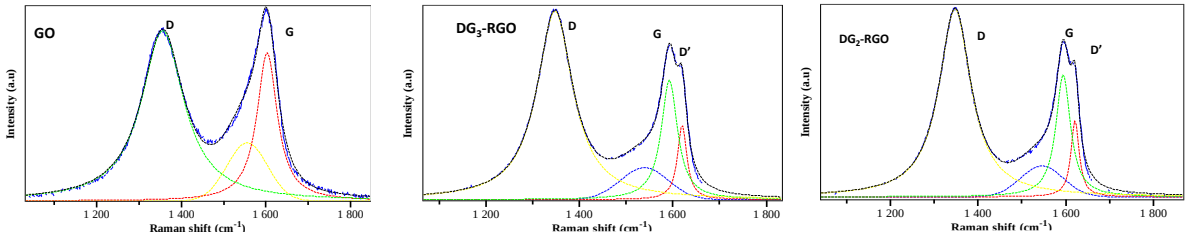

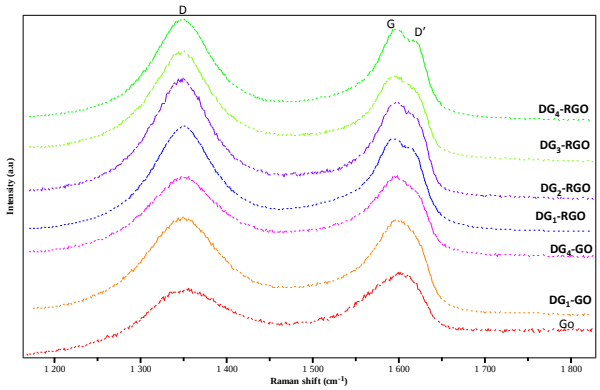

S9: XPS analysis

C 1s

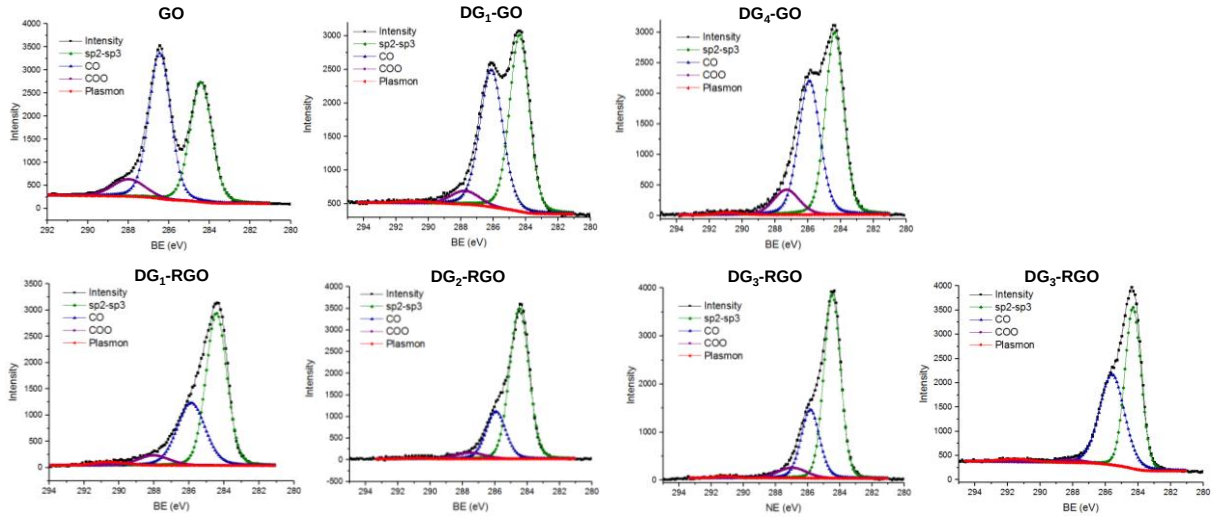

N 1s

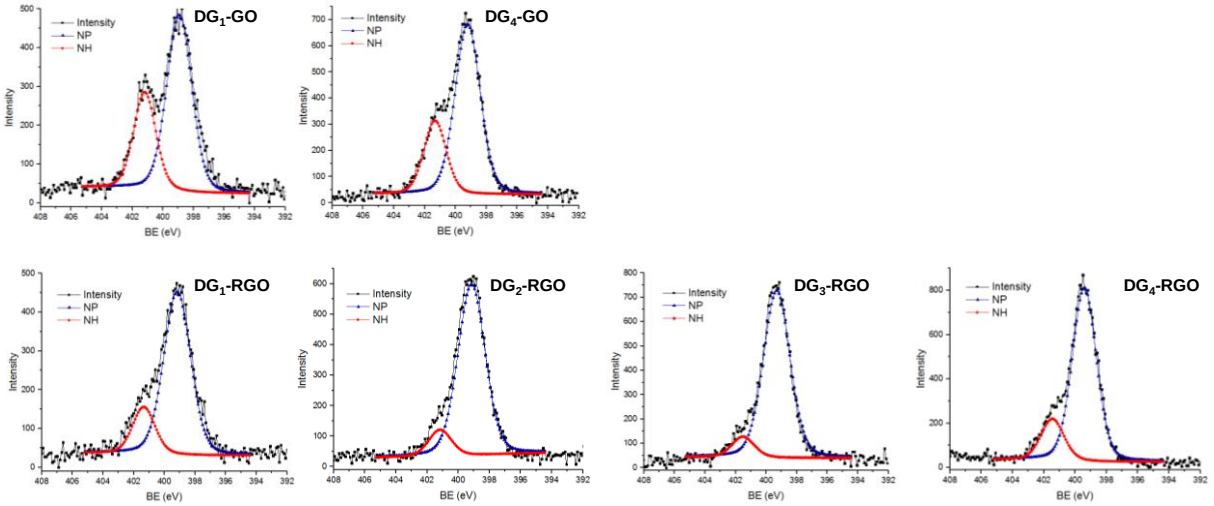

O 1s

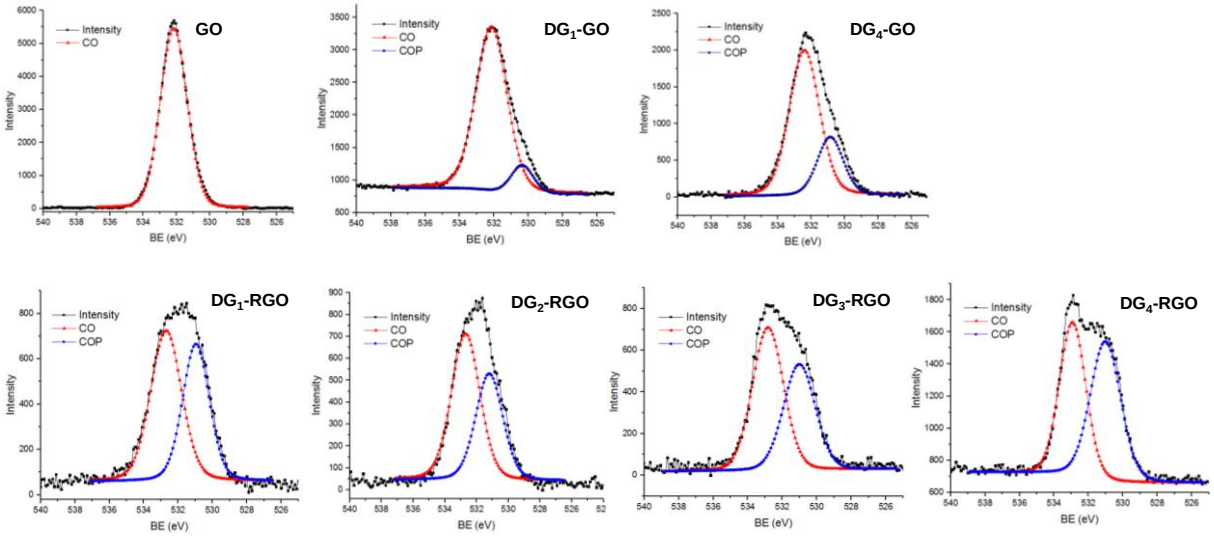

P 2p

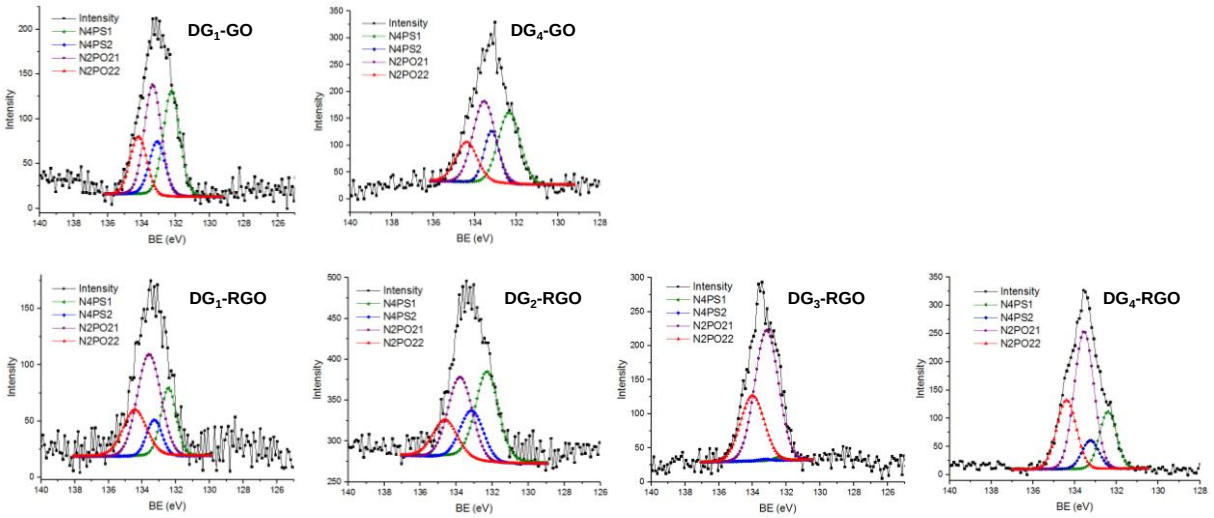
DG1-GO
DG4-GO
DG1-RGO
DG2-RGO
DG3-RGO
DG4-RGO
Intensity
N4PS1
N4PS2
N2PO21
N2PO22
BE (eV)

S 2p

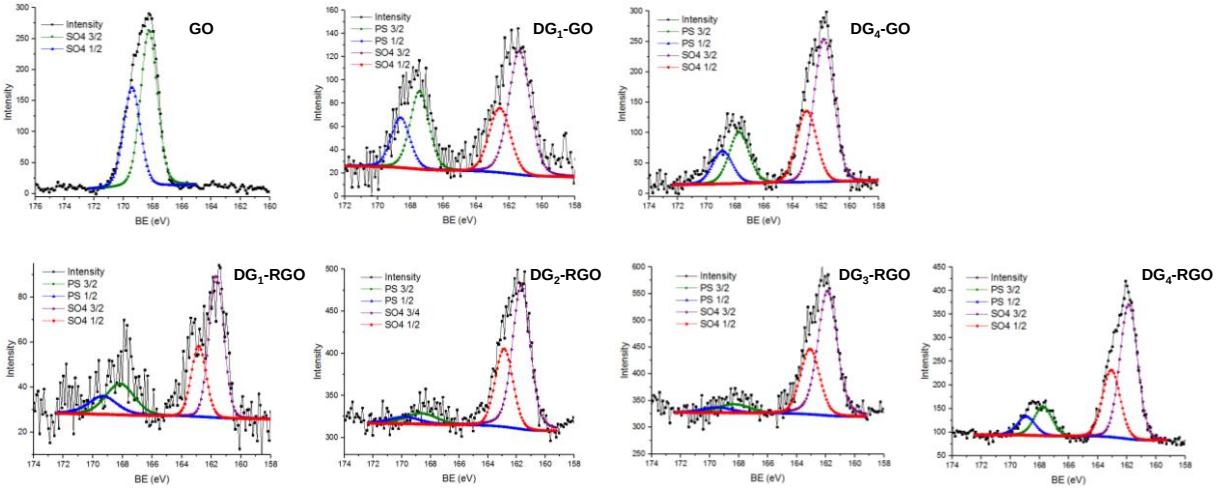
GO
DG1-GO
DG4-GO
DG1-RGO
DG2-RGO
DG3-RGO
DG4-RGO
Intensity
SO4 3/2
SO4 1/2
PS 3/2
PS 1/2
SO4 3/4
BE (eV)

Table 1S

Abscissa	C(sp2/sp3)	C(CO)	C(COO)	C(plasmon)	N(N-P)	N(C-NH)	O(C-O)	O(-O-P)	P(N4PS)	P(N2PO2)	S(SO4)	S(P=S)	Cl
GO	26.57	32.20	5.77	0.25	0	0	33.42	0	0	0	1.79	0	0
DG_1-GO	32.02	30.90	3.72	0.63	4.84	2.36	18.68	3.22	0.93	0.98	0.52	0.86	0.34
DG_4-GO	32.01	27.94	6.25	0.57	6.42	2.47	14.39	5.00	1.01	1.16	0.74	1.80	0.23
DG_1-RGO	45.61	25.87	4.67	1.65	6.16	1.46	6.74	5.29	0.58	1.25	0.23	0.48	0
DG_2-RGO	53.23	17.64	3.38	0.36	8.13	1.04	6.70	4.67	1.54	1.31	0.27	1.74	0
DG_3-RGO	47.76	20.54	4.65	0.59	9.40	0.96	6.19	4.69	0.03	2.49	0.31	2.41	0
DG_4-RGO	35.90	32.31	1.09	1.39	8.43	1.89	6.57	7.04	0.69	1.89	0.56	2.23	0

S10. Suggested mechanism.

A plausible mechanism taking place at the interface of the two phases can be reasonably suggested as follow: the terminal ternary diethyl-*N*-ethyl-ammonium chloride [(NH-$(CH_2)_2$-$N^+(Et)_2H,Cl^-$] induces ring opening of the epoxide by the nucleophilic attack of either its ammonium or its secondary amines[2] (that are also well exposed on the surface) resulting in the formation of carbon-nitrogen covalent bonding at the surface (Scheme 1). This is supported by the complete disappearance in **DG_n-GO** of the signal at 60 ppm in ^{13}C NMR, attributed to C-O-C bonds of the oxirane fragments. In parallel, the ternary alkylated ammoniums remain intact (in XPS: typical signal of quaternized nitrogen species -N^+- at 401.2 eV and the one of Cl^- species at 196.7 eV) or probably engaged in hydrogen-bonding with alcohols C-OH groups (the remaining signal at 70 ppm) and carboxylic acids.[3] In **DG_n-RGO**, a concerted mechanism allows deprotonation of ternary ammoniums to amines (no chloride or NH^+ were observed in XPS analyses) and elimination of hydroxylic groups (no signal was observed at 70 ppm). Notably, hydrazine treatment was executed herein at room temperature to avoid any competitive thermally-induced oxygen removal (thermal reduction) that may interfere with the reactivity of these materials.[4]

2. E. Araque, R. Villalonga, M. Gamella, P. Martínez-Ruiz, J. Reviejo and J. M. Pingarrón, *J. Mater. Chem. B*, 2013, **1**, 2289-2296.
3. As an experimental evidence, the electrolytic interaction of these ammoniums with alcohols and carboxylic acids affords flocculated solution. Upon reduction and in consistency with the deprotonation of ammoniums and alcohols, the suspension volume decreased significantly as a result of decreasing ionic interactions.
4. C. K. Chua and M. Pumera, *Chem. Commun.*, 2016, **52**, 72-75.

S11: TGA analysis